FEBRUARY 1983 LRP 218/83

SPECTRUM OF LOW-FREQUENCY, NON-AXISYMMETRIC OSCILLATIONS IN A COLD, CURRENT-CARRYING PLASMA COLUMN

K. Appert, J. Vaclavik and L. Villard

SPECTRUM OF LOW-FREQUENCY, NON-AXISYMMETRIC OSCILLATIONS IN A COLD, CURRENT-CARRYING PLASMA COLUMN

K. Appert, J. Vaclavik and L. Villard

Centre de Recherches en Physique des Plasmas
Association Euratom - Confédération Suisse
Ecole Polytechnique Fédérale de Lausanne
CH-1007 Lausanne / Switzerland

ABSTRACT

The spectrum of low-frequency, $m = \pm 1$ oscillations in a cold, collisionless, cylindrical plasma comprises the frequencies of the lowest radial eigenmodes and the surface modes of the fast magnetosonic wave, all the global eigenmodes of the Alfvén wave (ion cyclotron wave) and the Alfvén continuum. The spectrum of a homogeneous, currentless plasma cylinder is obtained from an analytical dispersion relation. This spectrum is compared with numerically obtained spectra of nonuniform plasmas with and without axial current. The connection of the MHD kink and internal kink instabilities with the global eigenmodes of the Alfvén wave is evidenced. Among all the modes of the magnetosonic wave which have frequencies in the Alfvén continuum, the ($m = -1$, $k < 0$)-surface mode is the best candidate for antenna-plasma coupling in an Alfvén Wave Heating scheme because its conversion layer is located well into the plasma interior.

I. INTRODUCTION

An axisymmetric or cylindrical bounded plasma with diffuse profiles, modelled by ideal magnetohydrodynamics (MHD) or by cold plasma theory, exhibits three distinct kinds of global, small amplitude oscillations: stable undamped eigenoscillations, purely or almost purely growing instabilities and damped oscillations at certain frequencies which lie in the Alfvén continuous spectrum. At first sight the appearance of a damping in a dissipationless system is astonishing. It can, however, be explained [1] by what is known as resonant absorption.

In ideal MHD the stable undamped eigenoscillations are radial eigenmodes of the slow and the fast magnetosonic wave [2] and of the Alfvén wave [3]. In cold plasma theory the slow magnetosonic wave does not exist, but the two others do. Most commonly the Alfvén wave is called ion-cyclotron wave in this case. Recently densely packed discrete oscillation frequencies have been observed on TCA Tokamak [4] and in numerical simulations [5] and have been interpreted as global eigenmodes of the Alfvén wave [3] or the ion-cyclotron wave.

An important class of fast-growing global instabilities which can be obtained from MHD are the current-driven external and internal kink instabilities [6,7]. These instabilities have many similarities with the global eigenmodes of the Alfvén wave [3]. Their existence, for instance, may be proven in the same way as Suydam's instability criterion [8].

We shall show that the kinks and the global eigenmodes of the Alfvén wave are the same modes but appearing at different axial wavenumbers k.

The damped oscillations have been named "surface waves" [9] or "surface eigenmodes" [10] because in a plane geometry they are confined to the neighbourhood of a plasma-vacuum interface. These modes are undamped if the interface is sharp [9,10]. The same should be true in a homogeneous plasma cylinder. In this case the surface wave should, in fact, be an eigenmode of the system and fall into the mentioned first class of oscillations, the stable undamped eigenoscillations. An essential part of the present investigation will be devoted to the "surface wave".

Apart from the interest in a unique nomenclature we have a strong interest in this mode in connection with Alfvén wave heating [11,12]. It is, in fact, this mode which is excited by an external antenna in the Alfvén Wave Heating scheme presently used [4]. It plays the role of the energy carrier as does the fast magnetosonic wave in the ICRF heating scheme. It will be shown that the surface wave is nothing else than the remnant of the first radial eigenmode of the fast magnetosonic wave. Since it has a radial wavelength of the order of the plasma radius it cannot be found by a WKB analysis which erroneously predicts cutoff at low frequencies.

It is the main goal of the present paper to provide a clear and simple picture of the low-frequency spectrum of a plasma column by

making evident the interconnections between modes with different names and different theoretical origin. Previous work has always been focussed on some partial aspect of the spectrum. Applying cold plasma theory to a homogeneous plasma cylinder Paoloni [13] remarked that the first radial eigenmode of the fast magnetosonic wave with the azimuthal wavenumber m = 1 did not suffer from cutoff at low frequencies. He did not, however, remark that the corresponding mode with m = -1 does also exist; its frequency lies very near to the eigenfrequencies of the Alfvén wave. Both modes have recently been described by Cramer and Donnelly [9] who investigated the dispersion relation in the case of a plane plasma-vacuum interface. The damping due to resonant absorption has also been calculated by these authors who have thereby generalized the ideal-MHD results of Lanzerotti et al. [14] to include finite-frequency effects. Their results are consistent with those obtained by Karney, Perkins and Sun [15].

The paper is structured as follows. In Section 2 the basic equations of our model are mentioned together with the definition of the notation used. In Section 3 an analytical dispersion relation is derived for a homogeneous plasma cylinder. This dispersion relation, which yields real frequencies, is solved analytically in some limiting cases. A numerical solution is obtained in all other cases. In Section 4 the basic equations are straightaway numerically integrated considering diffuse equilibrium profiles. The obtained dispersion relation yields complex frequencies in general. The resulting spectra are compared with the spectrum obtained in Section 3 and with results of the ideal-MHD stability theory. Finally, the main conclusions are drawn in Section 5.

II. BASIC EQUATIONS

We consider small-amplitude perturbations with frequencies much smaller than the lower-hybrid frequency in a cold current-carrying plasma. The plasma motion can then be described by the linearized equation of momentum transfer and the linearized Ohm law which includes the Hall term. We adopt a cylindrical geometry and assume that the equilibrium quantities are functions of radius r only. We may then take the time and space dependence of the perturbation quantities as $\exp[i\,(kz + m\theta - \omega t)]$, where k and m are the axial and azimuthal wavenumbers. When the equation of momentum transfer and the Ohm law are combined with the Maxwell equations (without displacement current) to yield a wave equation for the electric field, it is possible to retain the important effect of an axial equilibrium current by a systematic expansion to first order in the ratio of the equilibrium magnetic fields, $|B_{0\theta}/B_{0z}| \ll 1$. This wave equation takes the most elegant form when written in terms of the perturbed electric and magnetic fields $E_\perp$ and $B_\parallel$ [16]:

$$A\,\frac{1}{r}\,\frac{d}{dr}\,(rE_\perp) = Gk_\perp E_\perp + (A - k_\perp^2)\, i\omega B_\parallel \,, \tag{1}$$

$$A\,\frac{d}{dr}\,(i\omega B_\parallel) = (G^2 - A^2)\, E_\perp - Gk_\perp\, i\omega B_\parallel \,, \tag{2}$$

where

$$A = \varepsilon - k_\parallel^2 \,,\quad G = (\omega/\omega_{ci})\varepsilon - (2/r)B_{o\theta}k_\parallel \,, \tag{3}$$

and

$$\varepsilon = \frac{\omega^2 \rho_0}{1-(\omega/\omega_{ci})^2} .$$

All quantities here and throughout the paper are dimensionless. The usual ideal-MHD scales are used. Length and time are normalized to the minor radius a of the plasma column and the Alfvén transit time $a/c_A(r=0)$ respectively. The normalization of the magnetic fields $B_{\parallel}$ and $B_{0\theta}$, the electric field $E_{\perp}$ and the equilibrium mass density ρ_0 are respectively: B_{0z}= const, B_{0z} $c_A(r=0)/c$ and $\rho_0(r=0)$. Here c is the velocity of light. The local coordinate system $(r, \perp, \parallel)$ is defined by $\hat{r}$, $\hat{e}_{\perp} = \hat{e}_{\parallel} \times \hat{r}$ and $\hat{e}_{\parallel} = \vec{B}_0/B_0$, the caret denoting unit vectors. Consistent with this definition we have $k_{\parallel} = k + (m/r)B_{0\theta}$ and $k_{\perp} = m/r - kB_{0\theta}$.

We assume the plasma column to be surrounded by a vacuum region and by a perfectly conducting cylindrical shell of radius r_s, r_s = 1 being the limiting case of a fixed boundary plasma. The field equations in the vacuum region are given by eqs. (1) and (2) if the substitutions $k_{\parallel} = k$, $k_{\perp} = m/r$, $A = -k^2$ and $G = 0$ are used.

The eigenvalue problem can now be formulated: one looks for solutions of eqs. (1) and (2) in the plasma and the vacuum region, subject to the conditions that $E_{\perp}$ and $B_{\parallel}$ be continuous at the plasma-vacuum interface and that $E_{\perp}$ be zero at the shell.

The free parameters of the problem are r_s, m, k, ω_{ci} and the profiles of $\rho_0(r)$ and $B_{0\theta}(r)$. In physical terms k is usually determined by the toroidal wavenumber n, namely k = na/R, where a/R is the inverse aspect ratio of the torus in question. The dimensionless cyclotron frequency ω_{ci} does not depend on the magnetic field but is a measure of the total number of particles per unit length of the cylinder (or the torus):

$$\omega_{ci} = (4\pi)^{1/2} \frac{e}{c} a \left(\frac{n_{eo}}{m_i}\right)^{1/2} = 4.4\times10^{-8}\ a(cm)\ [n_{eo}(cm^{-3})z/\mu]^{1/2} \quad (5)$$

Here e is the elementary charge, m_i the ion mass, $\mu = m_i/m_{proton}$, z is the charge state and n_{eo} the peak electron density.

In the next two sections the eigenvalue problem is solved under different assumptions on the values of the free parameters.

III. HOMOGENEOUS PLASMA CYLINDER

The equations (1) and (2) can be combined into a simple Bessel equation for $B_{\parallel}$ when constant density, $\rho_0(r) = 1$, and zero axial current, $B_{0\theta} = 0$, are assumed:

$$\frac{1}{r} \frac{d}{dr}\left(r \frac{dB_{\parallel}}{dr}\right) + \left(k_r^2 - \frac{m^2}{r^2}\right) B_{\parallel} = 0, \quad (6)$$

where

$$k_r^2 = (A^2 - G^2)/A. \tag{7}$$

The quantities A and G are constant in this case. The solution in the plasma region is given by

$$B_{\parallel}(r) = C_1 J_m(k_r r), \quad r \leq 1 \tag{8}$$

if $k_r^2 > 0$ and by

$$B_{\parallel}(r) = C_1 I_m(|k_r| r), \quad r \leq 1 \tag{8'}$$

if $k_r^2 < 0$. In the vacuum region the solution reads

$$B_{\parallel}(r) = C_2 I_m(kr) + C_3 K_m(kr), \; 1 \leq r \leq r_s. \tag{9}$$

By using the three boundary conditions for $B_{\parallel}$ at $r = 1$ and $E_{\perp}$ at $r = 1$ and $r = r_s$ one eliminates the 3 unknown constants C_1, C_2 and C_3 and obtains the dispersion relation for k_r or for ω respectively:

$$\frac{Z_m'(|k_r|)}{Z_m(|k_r|)} + \frac{m}{|k_r|}\,\frac{G}{A} + \mathrm{sign}(k_r^2)\,\frac{|k_r|}{k}\,F_m(k, r_s) = 0. \tag{10}$$

The symbol Z_m denotes J_m if $k_r^2 > 0$ and I_m if $k_r^2 < 0$, the prime denotes the derivative with respect to argument,

$$F_m(k, r_s) = \frac{D_m(kr_s) I_m'(k) - K_m'(k)}{D_m(kr_s) I_m(k) - K_m(k)} \tag{11}$$

and

$$D_m (kr_s) = K_m' (kr_s)/I_m'(kr_s) \quad . \tag{12}$$

It is easy to solve eq. (10) numerically. A numerical solution is shown in Fig. 1. The free parameters are taken to be $\omega_{ci} = 2$ and $r_s = 1.5$ which are typical values of the TCA tokamak [4]. The eigenfrequencies $x = \omega/\omega_{ci}$ are shown for $m = +1$ and $m = -1$ as a function of k.

It is possible to obtain analytical solutions of eq. (10) in the limit $k \ll 1$. Then

$$F_m(k, r_s) \sim -k^{-1} (r_s^2 - 1)/(r_s^2 + 1)$$

and eq. (10) can be satisfied by $k_r \sim k$, $A \sim k^2$ or by $Z_m(k_r) \rightarrow 0$. For the case shown in Fig. 1 that last condition translates into $J_1(k_r) = J_1(\omega) = 0$, i.e. $\omega = j_{1,s}$, $s = 1, 2, \ldots$, where $j_{1,s}$ denotes the zeros of J_1. These are the frequencies of the radial eigenmodes of the fast magnetosonic wave (F) as they are known from ideal MHD [2]. The first zero, $j_{1,1} = 3.83$, leads to $x = \omega/\omega_{ci} = 3.83/2 = 1.91$. In Fig. 1 this mode is denoted with F_2 as the second radial eigenmode of the fast wave. As long as $k \lesssim 1$ this mode and all the higher ones are practically identical for $m = \pm 1$.

The first radial eigenmodes of the fast wave F_1 are obtained in the limit $k_r \sim k \rightarrow 0$. After expansion of the function Z_m, i.e.

$J_m'/J_m \sim m/k_r$, one obtains a quadratic equation for x; its solution is

$$\omega/\omega_{ci} = x = \alpha\ (1 + \mathrm{sign}(m)\ \alpha/2) \tag{13}$$

where

$$\alpha^2 = \frac{k^2}{\omega_{ci}^2}\ \left[\,|m|\ \frac{r_s^{\,2}+1}{r_s^{\,2}-1} + 1\right]. \tag{14}$$

For $m = \pm 1$ and $r_s \to \infty$ eq. (13) yields $\omega = \sqrt{2}\ k$ for very small k. This is the surface eigenmode frequency as given by ideal MHD theory [14]. In an MHD treatment (i.e. $\omega_{ci} \to \infty$) the two modes for $m = \pm 1$ behave identically and like an eigenmode of the fast wave. It seems therefore natural to identify the first radial eigenmode of the fast magnetosonic wave F_1 with the surface eigenmode S.

In Fig. 1 only the mode F_1, $m = -1$ has been labelled with S for the following reason. For small k the wave fields of F_1 are global functions as opposed to those of the surface wave in plane geometry where they are confined to the neighbourhood of the plasma-vacuum interface. It is only for $k \gtrsim 1$ that the mode F_1, $m = -1$ has surface-wave character as can be seen from Fig. 2. The mode F_1, $m = 1$ has global wave fields for all values of k. The surface-wave character of F_1, $m = -1$ in cylindrical geometry is clearly related to the fact that it merges with the Alfvén resonance $A = \varepsilon - k^2 = 0$, denoted by A_∞ (at $k = 1.5$ in the case of Fig. 1). The value of k where S and A_∞ merge depends on r_s as we shall see in Fig. 3.

Let us, however, first finish the discussion of Fig. 1 by describing the global eigenmodes of the Alfvén wave. These modes have often been called ion-cyclotron modes and very recently "discrete Alfvén waves" [4]. For small k they correspond to the combination $A \sim k^2$, $k_r \gtrsim 1$ satisfying eq. (10). As can be seen from Fig. 1 there is no physical interest to obtain solutions for $k \ll 1$ because the whole class is extremely densely packed; in the MHD limit the solutions are even infinitely degenerate. For $k > 1.5$ the eigenfrequencies of the lowest radial modes (only A_1, $m = \pm 1$ are shown; all the higher modes, A_s, $s > 1$, lie between A_1 and A_∞) are distinctly detached from the accumulation point A_∞. In the case shown, $r_s = 1.5$, $\omega_{ci} = 2$, the largest distances have been found around $k \approx 3.5$. The relative distances $(\omega_\infty - \omega_s)/\omega_\infty$ are 7.2 %, 3.2 % and 1.7 % for the modes $s = 1, 2, 3$, $m = -1$ and 3.6 %, 1.8 %, 1.1 % for $m = 1$. It is interesting to note, that the set of A_s, $m = -1$ seems to contain one mode more than $m = 1$, namely the mode A_1. All the other modes can, in fact, be put into a close one-to-one correspondence, $A_{s+1}(m=-1) \approx A_s(m=1)$, with respect to frequency and radial wavenumber k_r (not shown). At small k the surface mode S has been identified as an eigenmode of the fast wave; at high k it now appears as a part of the Alfvén wave. This is, however, from a purist's point of view, somewhat misleading. Strictly speaking, the mode lies always <u>above</u> A_∞ and should therefore not be identified with any eigenmode of the Alfvén wave.

A detailed investigation of the behaviour of the surface mode as a function of k and of the radius of the conducting shell, r_s, has

been made. The most striking result is shown in the upper part of Fig. 3. The radial wavelength k_r changes from real to imaginary as k grows. This fact explains the change (Fig. 2) from a global wave form at k = 0.4 to the surface wave form at k = 1.5: at k = 0.4 the eigenfunction for $B_{||}$ is given by $J_1(\sqrt{.15}\ r)$ whereas at k = 1.5 $B_{||}$ is given by a exponentially growing $I_1(|k_r|\ r)$. We note the strong effect of the conducting shell. The smaller the vacuum gap the higher are the axial phase velocities ω/k at small values of k (see lower part of Fig. 3). This fact is well described by eq. (14) which for $k \lesssim 0.4$ approximates the exact result within 10 %. From eq. (14) we conclude that the phase velocities of the mode F_1, m = 1 show the same tendency to increase, when the shell is approached to the plasma, as those of the surface wave. This effect has been described by Paoloni [13].

IV. DIFFUSE PROFILES

An alternative to the analytical dispersion relation, eq. (10), which is limited in its application to a homogeneous plasma cylinder, is a numerical dispersion relation which involves numerically determined fundamentals instead of the fundamentals J_m, K_m and I_m. The procedure is almost identical to that used in the calculation of the plasma loading impedance of an antenna surrounding the plasma [16] and will therefore not be described here. A similar procedure has been used by Karney et al. [15].

The first case shown here is (Fig. 4) that of a parabolic density profile, $\rho_0 = 1-0.99r^2$, with no axial current. As a consequence of the inhomogeneous density we now have a continuous spectrum of the Alfvén wave, in additon to discrete spectra. The continuum is given by eqs. (3) and (4) which for A = 0 yield

$$x_A(r) = x = |k_{\parallel}|/(\rho_0\omega_{ci}^2 + k_{\parallel}^2)^{1/2}. \qquad (15)$$

Note that in general both $k_{\parallel}$ and ρ_0 are functions of r. In Fig. 4, the lower and upper bound of the continuum, $x_A(r = 0)$ and x_A $(r = 1)$ respectively, are shown. In this figure $k_{\parallel} = k$ since $B_{0\theta} = 0$. Only the most important global modes (F_1, m = 1; S and A_1, m = -1) are represented. The frequencies of F_1 and S are somewhat higher than in Fig. 1, which is consistent with the fact that the average mass density for the parabolic profile is lower by a factor of two compared to the constant density profile. These modes F_1 and S therefore appear to be the eigenmodes F_1 and S which have been discussed in Fig. 1. However, for those values of k where they lie inside the continuum they are not solutions of the boundary value problem but merely time-asymptotic solutions of the corresponding initial value problem [1]. They have a complex frequency; the imaginary part is not shown in Fig. 4, but has been discussed in work related to Alfvén wave heating [9,10,15,16]. We are pleased to conclude from Fig. 4 that the modes F_1 and S ignore the above-mentioned subtle difference between an eigenmode and a mode immersed in a continuum.

This conclusion remains more or less true even in the much more complicated case of a current-carrying plasma cylinder (Fig. 5).

In addition to the parabolic density profile we have now included a peaked current profile $\sim (1-r^2)^4$ which results in $B_{0\theta} = .06\,[1-(1-r^2)^5]/r^2$. For an aspect ratio of 3.3 this field yields a safety factor of 1 on the axis and 5 at the plasma edge. The current makes the Alfvén continuum non-monotonous in r. We show therefore the lower bound min $x_A(r)$ of the continuum in addition to $x_A(r = 0)$ and $x_A(r = 1)$. Due to the current the solutions depend on the sign of k. We remark that the current merely shifts the two branches of the surface mode S by a small amount. The small shift in k is approximately equal to that observed for $x_A(r = 1)$. Apart from this small shift the dispersion relations of F_1 (not shown) and S seem to be unaffected by the current. In Figs. 4 and 5 they coincide up to values of k of the order of one. The deviation at higher values is accompanied by the appearance of an imaginary part of x (not shown) of the order of the real part.

The global eigenmodes of the Alfvén wave are distinctly separated from the continuum in the whole range of negative k values, but have completely disappeared from the positive range of k. In the negative range of k it looks as if the continuum, under the influence of the current, has withdrawn from the global Alfvén modes, whereas in the positive range of k the continuum has moved downwards hiding these modes.

The most striking new feature, however, is the existence of unstable eigenmodes. The graph has been obtained by plotting the imaginary part of x of the unstable eigenmodes; their real frequency

is practically zero as one would expect from MHD. The absolute value of the growth rates and the marginal stability points are not correctly given in Fig. 5 because the approximation used in the derivation of the basic equations, namely first order in $B_{0\theta}/B_{0z}$, is insufficient. A correct treatment would require at least quadratic terms [17]. The results are nevertheless easily interpretable. The mode A_1 is known in MHD as the external kink mode. In Fig. 5 its growth rate turns out to be roughly twice the correct MHD result. The range of instability is a bit too large in Fig. 5. Ideal MHD theory gives $0 \lesssim k \lesssim .3$. The modes A_s, $s \geq 2$, are called internal kink modes. They appear in the k-range where Suydam's stability criterion [8] is violated.

Inspecting Figs. 4 and 5 one can draw an important conclusion concerning Alfvén wave heating. Since the radial component of the Poynting vector $B_{\parallel} E_{\perp}$ is non-zero only for compressible plasma motions, i.e. $B_{\parallel} \neq 0$, one relies on the compressible fast magnetosonic wave for good antenna-plasma coupling at frequencies lying in the Alfvén continuum. In the low-frequency range the modes (F_1, $m > 0$) and $S = (F_1, m < 0)$ are the only candidates. It is a goal of the heating scheme to place the conversion layer (i.e. the Alfvén resonant surface) as near as possible to the center of the plasma. From Fig. 4 we learn that the surface mode has its resonant surface nearer to the center than the fast mode F_1. We select therefore the surface mode S. An inspection of Fig. 5 then leads us to choose the mode with a negative value of k, i.e. the mode whose helicity has the same sign as that of the equilibrium magnetic field.

V. CONCLUSIONS

On comparing the spectra of a homogeneous currentless plasma cylinder with those of nonuniform plasmas with and without axial current we have presented a unified and simple picture of the low-frequency modes in a tokamak. We have shown that the lowest radial eigenmodes of the fast magnetosonic wave have a distinctly different character depending on the sign of the azimuthal wavenumber m. In one case it is the eigenmode F_1, known from MHD, whose frequency varies from zero to infinity when the axial wavenumber k varies in the same range. In the other case the frequency does not exceed the ion-cyclotron frequency. This mode of the magnetosonic wave can assume the character of a surface wave if certain conditions are fulfilled. We have also shown that the subtle mathematical difference between an eigenmode and a mode immersed in a continuum does not have any consequence as far as the real dispersion properties of the mode are concerned. This fact facilitates the discussion of how the energy is coupled from the antenna to the plasma in an Alfvén Wave Heating scheme.

Moreover, we have shown that the kink and internal kink instabilities are identical with the global eigenmodes of the Alfvén wave, i.e. the modes which have also been called "discrete Alfvén waves" or ion-cyclotron modes. Implicitly we have shown that the classical scheme of Alfvén Wave Heating does not rely on the resonant absorption of a kink mode as we have claimed in earlier publications [18] but on the resonant absorption of a fast magnetosonic surface mode [10]. We

have been misled by the fact that the kink mode is clearly connected to the first radial eigenmode of the fast magnetosonic wave in the ideal-MHD spectrum of a current-carrying plasma with uniform [2] or almost uniform [2,19] density. For realistic density profiles we have never found a connection betweeen the kink and the magnetosonic surface modes.

Some of the features of the surface wave have been noted by G.A. Collins in his thesis [20].

ACKNOWLEDGEMENTS

The incentive for this investigation came from an enlightening discussion with Y. Amagishi to whom we are very grateful. We have benefited from interaction with J. Adam, G. Collins, R. Gruber and F. Troyon.

This work has been supported by the Ecole Polytechnique Fédérale de Lausanne, by the Swiss National Science Foundation and by Euratom.

REFERENCES

1 Z. Sedlacek, J. Plasma Phys. 5, 239 (1971).

2 M.S. Chance, J.M. Greene, R.C. Grimm and J.L. Johnson, Nucl. Fusion 17, 65 (1977).

3 K. Appert, R. Gruber, F. Troyon and J. Vaclavik, Plasma Phys. 24, 1147 (1982).

4 A. de Chambrier, P.A. Duperrex, A. Heym, F. Hofmann, B. Joye, R. Keller, A. Lietti, J.B. Lister, A. Pochelon and W. Simm, Phys. Letters 92A, 279 (1982).

5 D.W. Ross, G.L. Chen, and S.M. Mahajan, Phys. Fluids 25, 652 (1982).

6 J.A. Wesson, Proc. Seventh Europ. Conf. on Contr. Fusion and Plasma Phys., Lausanne, 1975, Vol. II, p. 102.

7 G. Bateman, "MHD Instabilities", MIT Press, Cambridge, Massachusetts, 1978.

8 B.R. Suydam, IAEA Geneva Conf. 31, 157-159 (1958).

9 N.F. Cramer and I.J. Donnelly, "Fast and ion-cyclotron surface waves at a plasma-vacuum interface", submitted to Plasma Physics.

10 L. Chen and A. Hasegawa, Phys. Fluids 17, 1399 (1974).

11 A. Hasegawa and L. Chen, Phys. Rev. Lett. 32, 454 (1974).

12 B. Balet, K. Appert and J. Vaclavik, Plasma Phys. 24, 1005 (1982).

13 F. Paoloni, Phys. Fluids 18 (1975) 640.

14 L.J. Lanzerotti, H. Fukunishi, A. Hasegawa, and Liu Chen, Phys. Rev. Letters 31, 624 (1973).

15 C.F.F. Karney, F.W. Perkins, and Y.-C. Sun, Phys. Rev. Lett. 42, 1621 (1979).

16 K. Appert and J. Vaclavik, Lausanne Report LRP 207/82, 1982, accepted for publication in Plasma Phys.

17 M.N. Bussac, R. Pellat, D. Edery and J.L. Soulé, Phys. Rev. Letters 35, 1638 (1975).

18 K. Appert, B. Balet, R. Gruber, F. Troyon, T. Tsunematsu and J. Vaclavik, Proc. 2nd Joint Grenoble-Varenna Int. Symp. on Heating in Toroidal Plasmas, 1980, Vol. II, p. 643.

19 A. Pochelon, R. Keller, F. Troyon and R. Gruber, Proc. 7th Europ. Conf. on Contr. Fusion and Plasma Phys., 1975, Vol. I, p. 157.

20 G.A. Collins, private communication, 1983.

FIGURE CAPTIONS

Fig. 1 The frequency spectrum, $x = \omega/\omega_{ci}$, of a currentless plasma cylinder with uniform density as a function of the axial wavenumber k. For the two azimuthal wavenumbers $m = \pm 1$, the lowest radial modes of the fast magnetosonic wave are designated as F_1 and F_2, those of the Alfvén wave as A_1. The broken line A_∞ represents the accumulation point of the eigenfrequencies of the Alfvén wave. The symbol S stands for "surface eigenmode".

Fig. 2 The wave field of the surface eigenmode in a currentless plasma cylinder with uniform density as a function of radius. The three figures for different axial wavenumber k illustrate the metamorphosis of the global mode F_1, $m = -1$ (at $k = 0.4$) into a surface-confined mode S(at $k = 1.5$).

Fig. 3 The radial wavenumber squared, k_r^2, and the frequency, $x = \omega/\omega_{ci}$, of the surface mode as a function of the axial wavenumber k for different shell positions r_s. The accumulation point of the eigenfrequencies of the Alfvén wave, A_∞, is shown with a broken line.

Fig. 4 The frequency spectrum, $x = \omega/\omega_{ci}$, of a currentless plasma cylinder with parabolic density profile as a function of the axial wavenumber k. The upper and lower bounds of the Alfvén continuum are shown with broken lines, $x_A(r=1)$ and $x_A(r=0)$ respectively. Only the most important modes, F_1, S and A_1 are shown.

Fig. 5 The frequency spectrum, $x = \omega/\omega_{ci}$, of a current-carrying plasma cylinder with a parabolic density profile as a function of the axial wavenumber k. The Alfvén continuum is characterized by the values of x_A in the center $r = 0$ and at the plasma edge, $r = 1$. In the region $-0.8 < k < 0.3$ $x_A(r)$ is not monotonous in r and has a minimum which is also shown. The stable global eigenmodes of the Alfvén wave are connected with the unstable kink (A_1) and the internal kink (A_2, A_3) modes. The surface mode (S) is only slightly affected by the current.

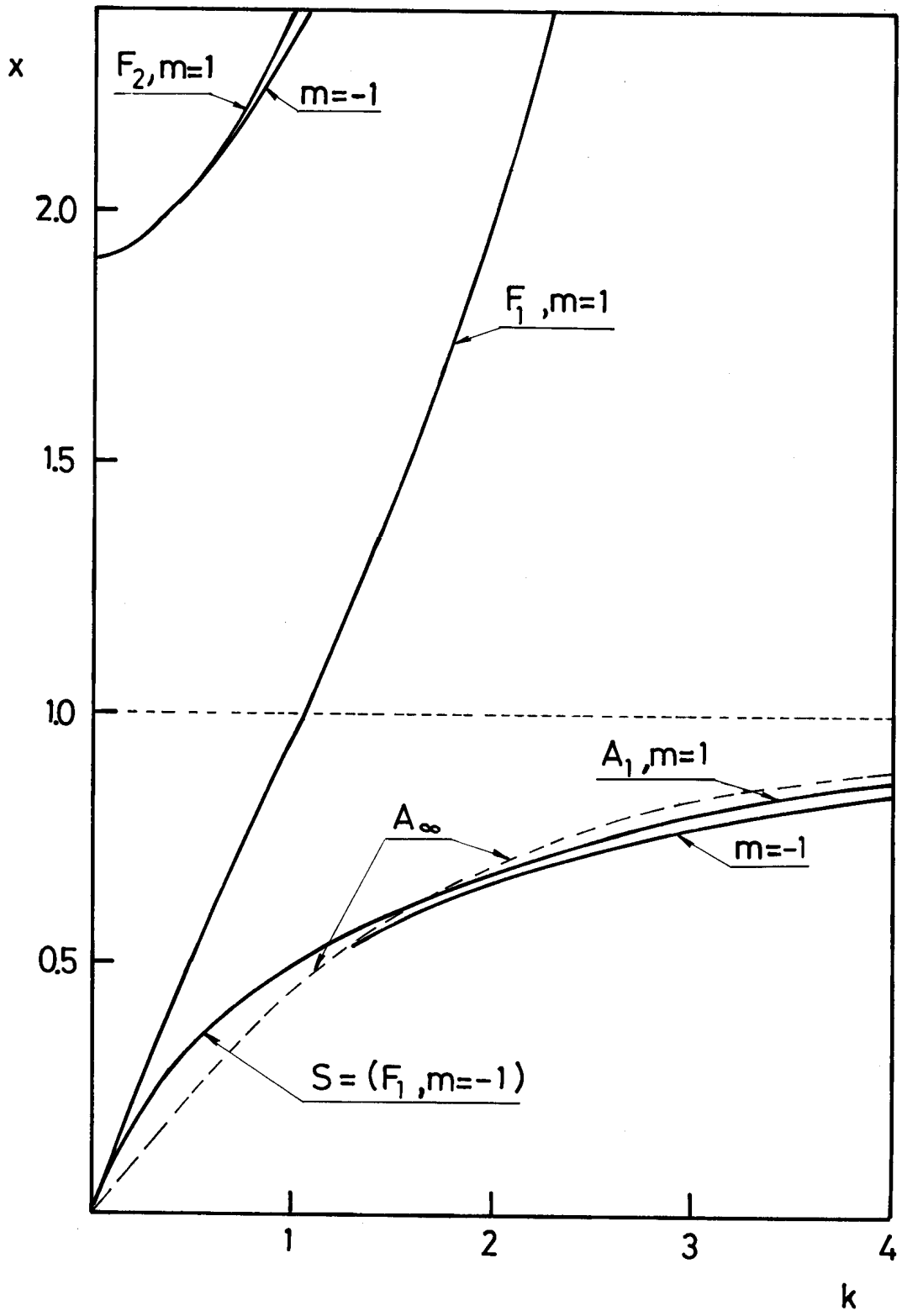

FIG. 1

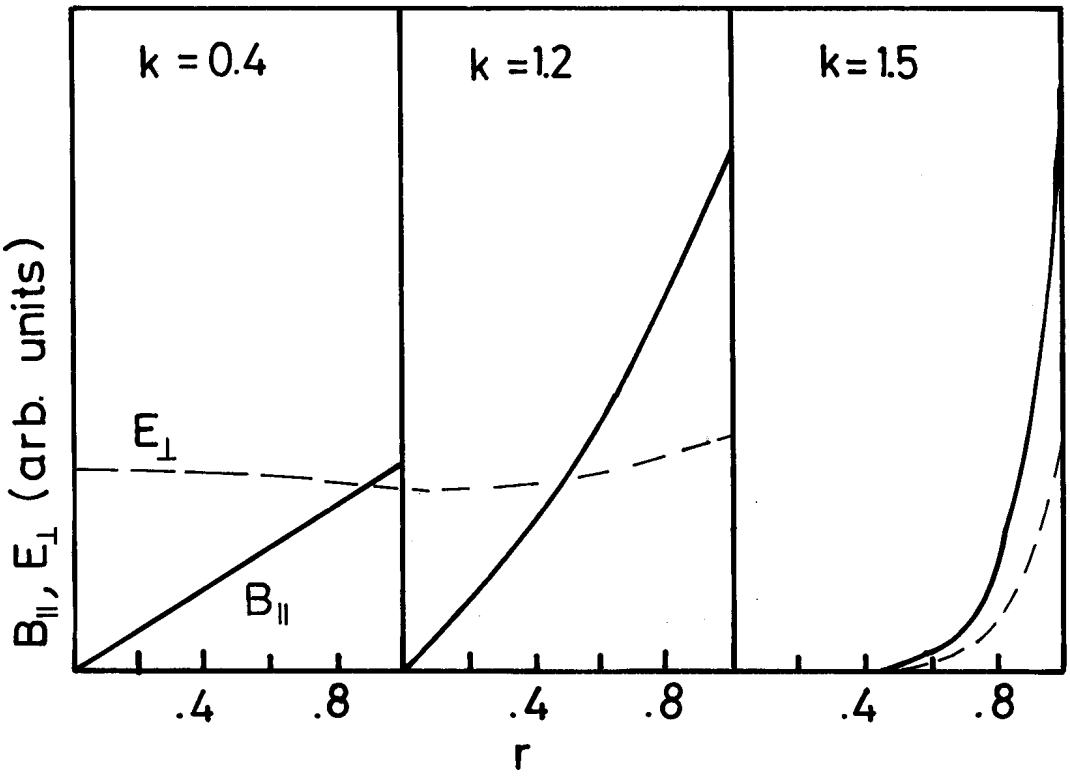
k = 0.4
k =1.2
k= 1.5
$E_\perp$
$B_\parallel$
$B_\parallel, E_\perp$ (arb. units)
.4
.8
.4
.8
.4
.8
r

FIG. 2

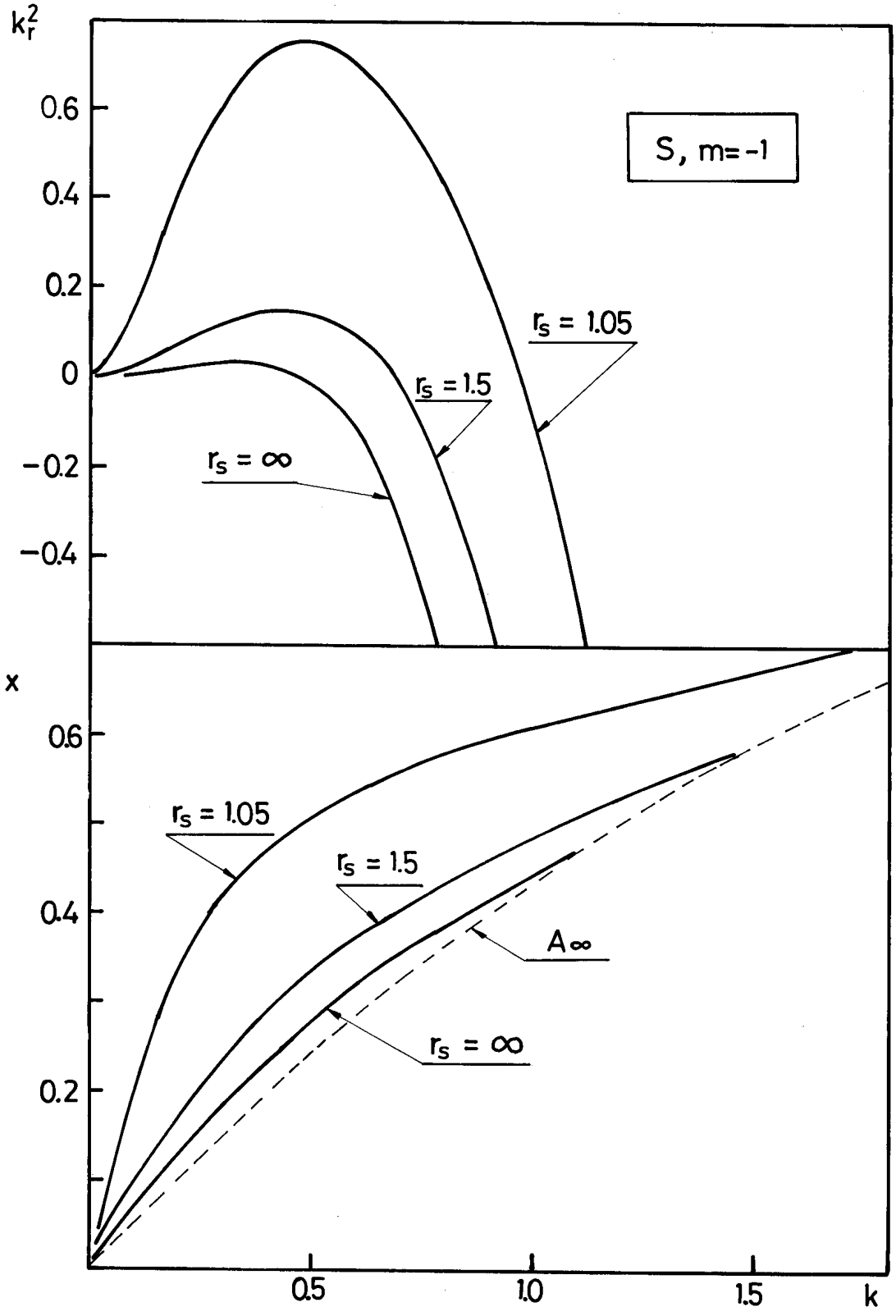
k_r^2
0.6
0.4
0.2
0
−0.2
−0.4
S, m=-1
r_s = 1.05
r_s = 1.5
r_s = ∞
x
0.6
0.4
0.2
r_s = 1.05
r_s = 1.5
A∞
r_s = ∞
0.5
1.0
1.5
k

FIG. 3

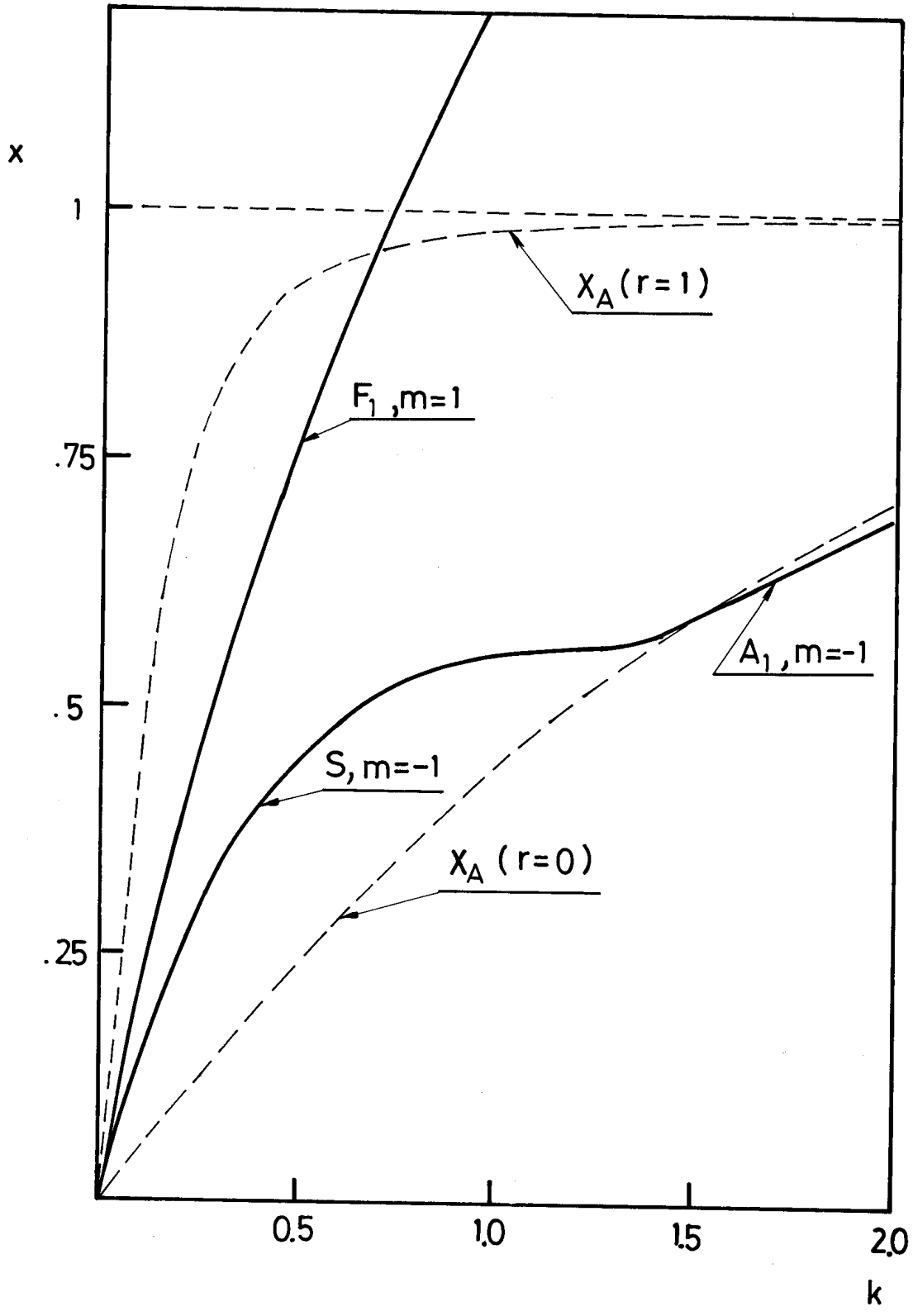

FIG. 4

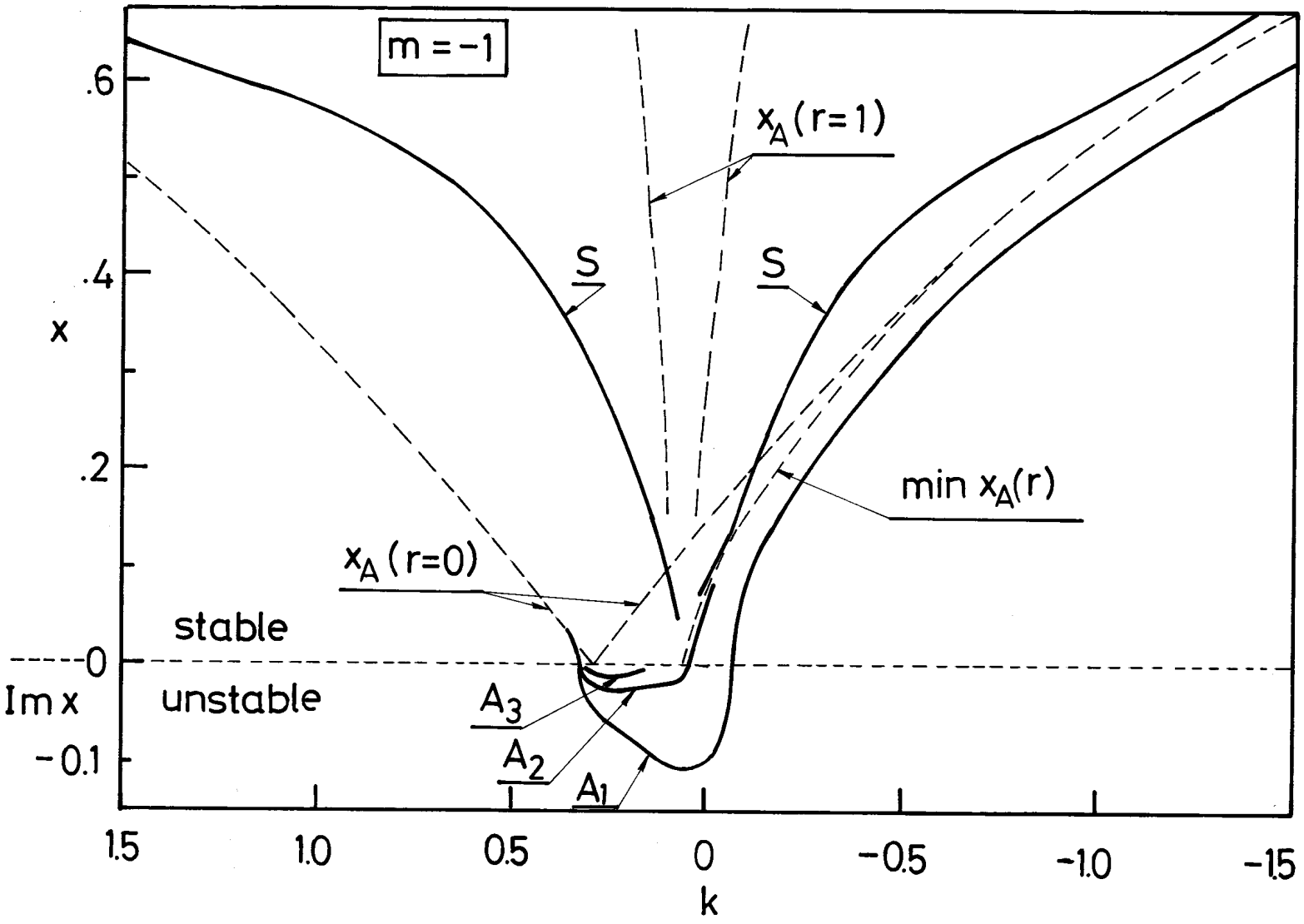
m = -1
.6
.4
.2
0
-0.1
x
Im x
$x_A(r=1)$
S
S
$x_A(r=0)$
min $x_A(r)$
stable
unstable
A_3
A_2
A_1
1.5
1.0
0.5
0
-0.5
-1.0
-1.5
k

FIG. 5